

Application of the modified approach of Finite Element Method for determining the displacement current distribution in nonlinear magnetic circuits

Abstract. Within this article the multistage approach of Finite Element Method combined with the Fixed-Point Method and Harmonic Balance Method has been presented and discussed. In the paper the analysis of the field model of a high-frequency transformer has been conducted. Obtained results enables the complex analysis of displacement currents distribution in a converter core and also estimation of the phenomena impact on operate states of the transformer.

Streszczenie. W ramach niniejszego artykułu omówiona i zaprezentowana została wielostopniowa metoda elementów skończonych, w której wykorzystane zostały Metody Punktu Ustalonego (Fixed - Point Method) oraz Metody Bilansu Harmonicznych (Harmonic Balance Method). W pracy wykonano i poddano analizie model połowy transformatora wysokiej częstotliwości. Przeprowadzone obliczenia umożliwiły zobrazowanie rozkładu prądów przesunięcia dielektrycznego w rdzeniu oraz ocenę wpływu zjawiska na pracę przetwornika elektromagnetycznego. (Zastosowanie zmodyfikowanego podejścia Metody Elementów Skończonych do wyznaczania rozkładu prądu przemieszczenia w nieliniowych obwodach magnetycznych)

Keywords: Displacement currents, transformer, Fixed-Point Method, Harmonic Balance Method

Słowa kluczowe: Prądy przesunięcia dielektrycznego, Metoda punktu ustalonego, metoda harmonicznego balansu,

Introduction

For over two decades, a persistent trajectory toward continuous miniaturization has manifested itself within the domain of electrical engineering. The evolution involves the ongoing development of increasingly compact device prototypes, concomitantly upholding elevated standards of power and efficiency. It is imperative to underscore that the progress of the miniaturization process is contingent upon not only the innovation magnetic materials [1,2] but, crucially, the advancement in power electronics and the growth in the frequency of power sources for converters [3,4]. Presently, efforts are underway to innovate electromagnetic converters by harnessing conductivity currents and dielectric displacement currents, as exemplified by the high-frequency capacitive-inductive transformer system pioneered by a team of researchers from the Military University of Technology in Warsaw [6]. The discernible impact of dielectric displacement currents on the electromagnetic field distribution is already observable in converters exposed to voltages at frequencies in the order of several dozen kilohertz, with particular prominence in regions including a core made of composite material or winding conductors [7]. A comprehensive review of existing literature reveals numerous instances where the analysis of displacement current distribution is discussed [8,9]. However, limited attention has been directed towards field analysis using the Finite Element Method (FEM). Certain research groups adopt Darwin's formulation for the examination of electric and magnetic fields in electromagnetic converters utilizing a model akin to the proposed one, though distinct in its omission of the rotational components of the displacement current densities [10,11]. In the domain of electrical engineering, there are a few commercial software options enabling the analysis of displacement current distribution; however, their output often focuses solely on displacement current densities [12]. Furthermore, implementing non-sinusoidal waveforms in a current or voltage source proves to be challenging in many commercial software. Another notable difficulty inherent in commercial software is the escalating computational time associated with higher saturation stages in electromagnetic converters. This

phenomenon is attributed to the time-domain method prevalent in many nonlinear solvers, coupled with a non-constant time step. In response to these challenges, the authors have embarked on research efforts aimed at formulating a comprehensive computational system designed to help engineers in the computation and simulation of electromagnetic phenomena. The intended numerical algorithm aims to provide fast and accurate results for analysing the distribution of electromagnetic fields in converters, incorporating the subtle influence of eddy and displacement currents on the distortion of magnetic flux distribution. The fusion of the Harmonic Balance Method (HBM) and the Fixed-Point Method (FPM) is anticipated to reduce convergence time, particularly in regions characterized by high saturation stages. The authors anticipate that the proposed computational system will streamline and accelerate the simulation and calculation processes for electromagnetic converters during the design process. Furthermore, the incorporation of displacement current effects in electromagnetic core and winding areas is envisioned to yield refined insulation selection and a more precise approximation of temporal-life considerations. This research builds upon antecedent studies published in [12], with a principal focus on the analysis of the impact of output resistance (R_0) on the input and output waveforms of the high-frequency transformer.

Methodology

In the open literature, there are many FEM-based formulations; however, only a few are suitable to use in the analysis of the distribution of displacement current. In the case of electromagnetic converters, areas with displacement current can be coherent – inter-core capacitance – or non-coherent - inter-turns capacitances. In the project, the Authors consider formulations that describe vectors of current density and magnetic flux in finite elements using interpolation functions of a facet element, whereas for a description of a vector of a gradient of scalar potential - interpolation functions of an edge element. Facet values of vectors representing the magnetic flux have been expressed by edge values of vector magnetic potentials \mathbf{A} ,

whereas edge values of a gradient of scalar electric potential V have been described using nodal values of the appropriate scalar potential. The elaborated algorithm uses two types of equation groups for FEM, i.e.: (a) equations for edge element method (EEM); and (b) equations for nodal element method (NEM). According to the open literature, the Authors consider the EEM equations the loop equations of the facet network (FE), whereas the NEM equations are the nodal equations of the edge network (EN) [13,14,15]. Moreover, the finite elements circuit models for FE and EN networks adapted to the analyses of the field, including displacement currents, have been elaborated. In order to simplify the calculation while maintaining a high convergence level, instead of a 3D full-field model, the axisymmetric 2D model has been used in the calculations. In the Figure 1, the axisymmetric model of the transformer has been presented.

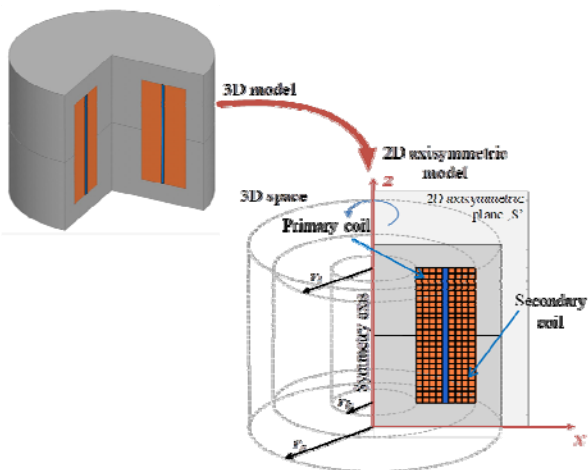


Fig.1. 2D axisymmetric model of the transformer

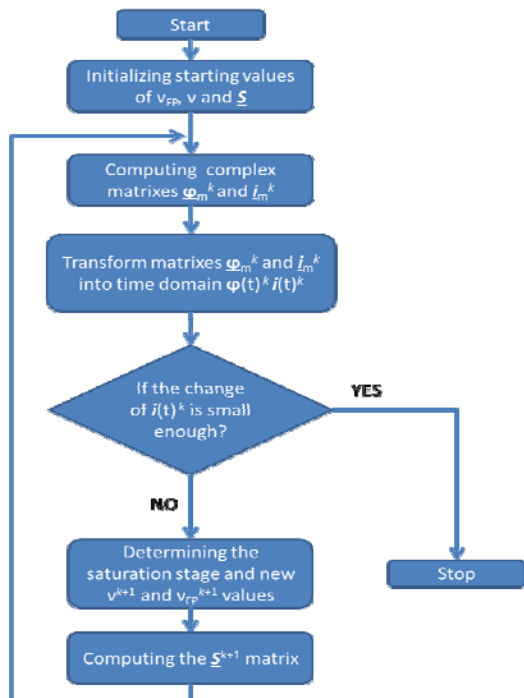


Fig.2. The reluctance-conductance-capacitance network model [12]

In the further stage of the research, the coupled reluctance-conductance-capacitance network model, shown in Figure 3, and the appropriate \mathbf{A} - V method equations have been introduced in order to determine the final

equations system with the application of HBM and FPM methods. Then the Authors have associated equations from both equation groups of EEM and NEM for electric field with elaborated circuit models for the FE and EN networks describing the magnetic field distribution, thus creating coupled field models. In the proposed formulas, both Fixed-Point Method and Harmonic Balance Method have been introduced [16,17]. On the basis of the final equation system, the numerical algorithm has been elaborated.

Due to its iterative character and separate calculation for each higher harmonics, the HBM method is suitable for the application of parallel computing; thus, in comparison to the standard time-domain approach using the coupled method of FPM and HBM enables to limit the convergence time significantly, especially for analysis of high-saturated areas.

Elaborated algorithm

In the case of a simply electromagnetic converter like a discussed transformer, the required equation system is built of two equations, i.e., the equation for the magnetic circuit and the equation for the electric circuit of the primary and secondary windings (1). To determine the distribution of eddy and displacement currents the relationship between the current density vector \mathbf{J} , vector magnetic potential \mathbf{A} and the gradient of the scalar potential V have been used [18].

$$(1) \begin{cases} \mathbf{R}_{\mu\omega}(\mathbf{v}) \cdot \boldsymbol{\varphi} = \mathbf{k}_o^T \mathbf{N}(\mathbf{z}_1)_k i_{c1} + \mathbf{k}_o^T \mathbf{N}(\mathbf{z}_2)_k i_{c2} - \mathbf{G} \frac{\partial}{\partial t} \boldsymbol{\varphi} - \mathbf{C} \frac{\partial^2}{\partial t^2} \boldsymbol{\varphi} \\ u_z = R_{c1} \cdot i_{c1} + \frac{\partial}{\partial t} (\mathbf{z}_1^T \mathbf{N}^T \mathbf{k}_o \boldsymbol{\varphi}) \\ 0 = (R_0 + R_{c2}) \cdot i_{c2} + \frac{\partial}{\partial t} (\mathbf{z}_2^T \mathbf{N}^T \mathbf{k}_o \boldsymbol{\varphi}) \end{cases}$$

According to our research object the Harmonic Balance Method could be described as follow:

$$(2a) \quad \mathbf{S} \cdot x(t) + \mathbf{M} \frac{\partial x(t)}{\partial t} + \mathbf{D} \frac{\partial^2 x(t)}{\partial t^2} = y(t)$$

$$(2b) \quad x(t) \cong \text{Re} \left\{ X_0 + \sum_{m=1}^M X_k e^{jm\omega t} \right\}$$

$$(2c) \quad y(t) \cong \text{Re} \left\{ Y_0 + \sum_{m=1}^M Y_k e^{jm\omega t} \right\}$$

According to equations (2b) and (2c), the HBM requires the Fourier transform to determine the values of individual higher harmonics. These values are used in further calculations to estimate the saturation stage and the resulting distortion of electromagnetic field distribution.

In order to introduce the Fixed-Point Method, only two simple equations need to be applied.

$$(3a) \quad v = v_{FP} + (v - v_{FP})$$

$$(3b) \quad \mathbf{R}_{\mu\omega}(\mathbf{v}) = \mathbf{R}_{\mu\omega}(v_{FP}) + \mathbf{R}_{\mu\omega}(v - v_{FP})$$

where: v is the magnetic reluctivity and v_{FP} is the fixed-point parameter

Using above-mentioned methods equations, the equation (1) can be transformed into the final matrix form equation system of (4).

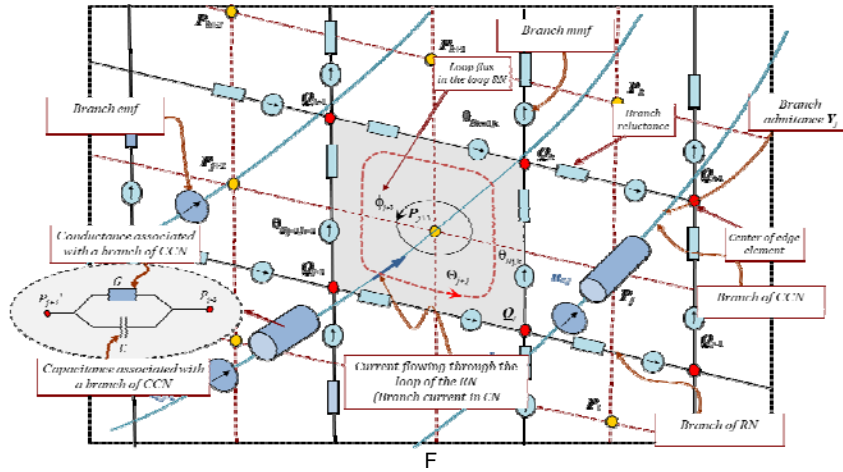


Fig.3. The reluctance-conductance-capacitance network model [12]

$$(4) \quad \begin{bmatrix} \mathbf{R}_{\mu 0}(v_{FP}^k) + j\omega \mathbf{M} & -\mathbf{k}_o^T \mathbf{N}(z_1)_k & -\mathbf{k}_o^T \mathbf{N}(z_2)_k \\ j\omega \mathbf{M}(z_1)_k^T \mathbf{N}^T \mathbf{k}_o & R_{c1} & 0 \\ j\omega \mathbf{M}(z_2)_k^T \mathbf{N}^T \mathbf{k}_o & 0 & R_0 + R_{c2} \end{bmatrix} \cdot \begin{bmatrix} \phi_m^{k+1} \\ i_{c1,m}^{k+1} \\ i_{c2,m}^{k+1} \end{bmatrix} = FFT \left\{ \begin{bmatrix} -\mathbf{R}_{\mu 0}(v^k - v_{FP}^k) \cdot \phi^k(t) - C \frac{\partial^2 \phi^k(t)}{\partial t^2} \\ u_z(t) \\ 0 \end{bmatrix} \right\}$$

where: the $\mathbf{R}_{\mu 0}$ is the loop reluctance matrix, ϕ is the vector of the edge values of potential \mathbf{A} , \mathbf{N} is the matrix that transposes the values in loops around edges to the values in loops that are ordered to centres of the element faces, $(z_1)_k$ and $(z_2)_k$ represent the number of coil turns arrange in the edge element space-matrix, i_{c1} and i_{c2} are the input and output currents respectively, \mathbf{G} and \mathbf{C} constitute the matrix of the branch conductances and the matrix of the branch capacitances of elaborated network model, u_z is the supply voltage of the primary winding, R_{c1} and R_{c2} are respectively the primary and secondary resistance values, R_0 constitutes the load resistance connected to the secondary winding, M is the maximal analysed order of higher harmonics, ω is the electrical pulsation of the fundamental harmonic of the supply voltage waveform, m is the order of the considered harmonic and k constitutes the actual iteration step of the calculation process.

To enhance comprehension of the Harmonic Balance Method, a simplification of the equation system (4) has been carried out, reducing its right-hand side to the \mathbf{S} matrix. The streamlined flow of the calculation process is visually represented in Figure 2 through a simplified block diagram. The magnetic flux matrix and current matrix are derived by utilizing initial values of magnetic permeability v , fixed-point parameter v_{FP} , and the \mathbf{S} matrix. Subsequently, new values of magnetic permeability v and v_{FP} for elements are determined based on the magnetic flux density \mathbf{B} for individual elements, calculated from the acquired magnetic fluxes. The methodology for determining the v and v_{FP} parameters has been extensively explained in [11]. Following the application of these determined values to equation (4), the calculation of $\mathbf{S}_{k+1}(t)$ ensues. Thereafter, the Fast Fourier Transform (FFT) is employed to convert the matrix $\mathbf{S}_{k+1}(t)$ into the complex form $\underline{\mathbf{S}}$. This procedure will be repeated until obtaining the satisfactory convergence level.

In the research, Authors have calculated two separate 2D axisymmetric field models. In the first one the output resistance R_0 equals to 5Ω has been applied and in the second one - 25Ω . In both model the supply voltage of 10V and frequency of 100 kHz has been applied. The displacement current distribution analysis has been carried out only in the region of the core. However, in the near

future it is expected to start research on displacement current distribution in windings area.

The analysed transformer's dimensions have been shown in Figure 4. For the material of the core the alloy powder F3000 has been chosen. In order to simplify the simulation, process the windings area has been approximated as a solid region.

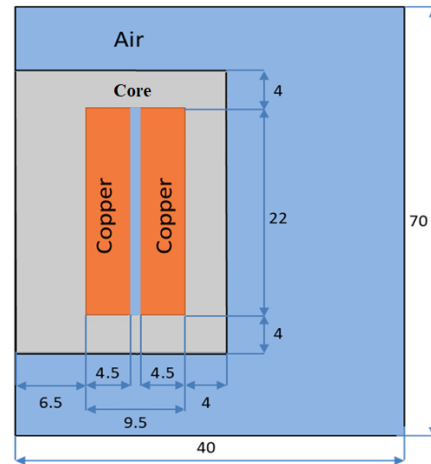


Fig.4. The geometry dimensions of the 2D transformer in millimetres.

The primary and secondary current waveforms are shown in Figures 5a and 5b. It can be easily concluded that increase in output resistance results in the time constant reduction of an RL circuit and thus the output current waveforms form the square waveform.

In Figures 6 and 7 the displacement current waveforms and distributions have been presented. The impact of value change of secondary winding resistance R_0 on displacement current distribution is much smaller than for input and output currents. In case of square electromotive force (EMF) the displacement current forms a series of peaks of value much higher than in case of sinusoidal voltage source. Analysing Figure 6b could yield additional intriguing conclusion, particularly regarding the opposite sign of displacement current values for two selected elements at the same time samples.

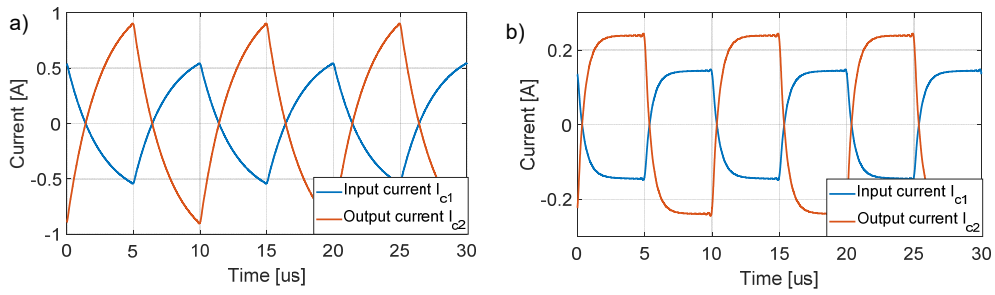


Fig 5. Transformer input and output currents i_c and i_{c2} waveforms for a) $R_0 = 5\Omega$ and b) $R_0 = 25\Omega$

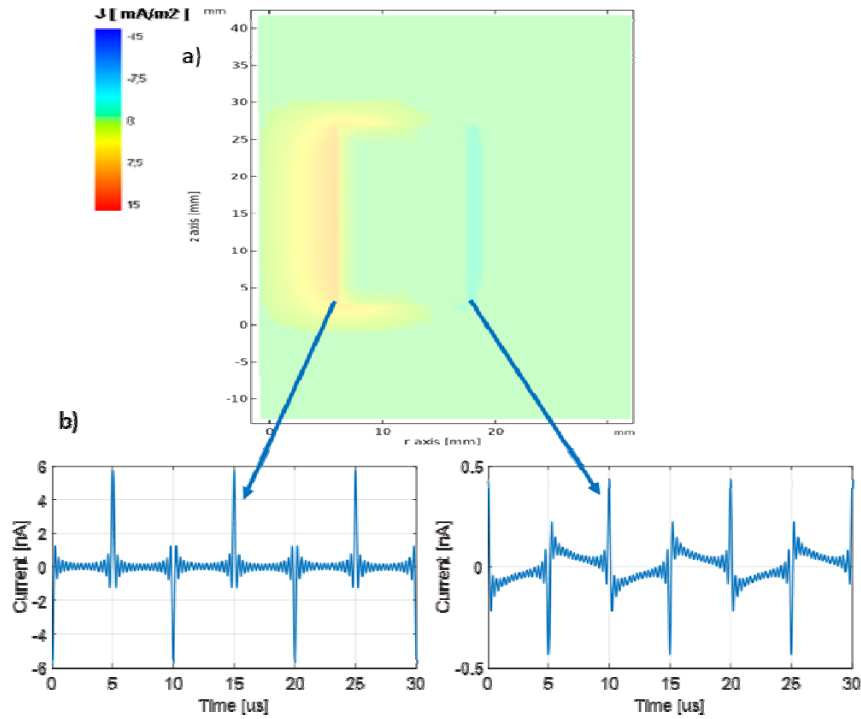


Fig. 6. Displacement current a) distribution for time $t = 5\mu s$, b) waveforms for selected elements in the ferrite core for $R_0 = 5\Omega$

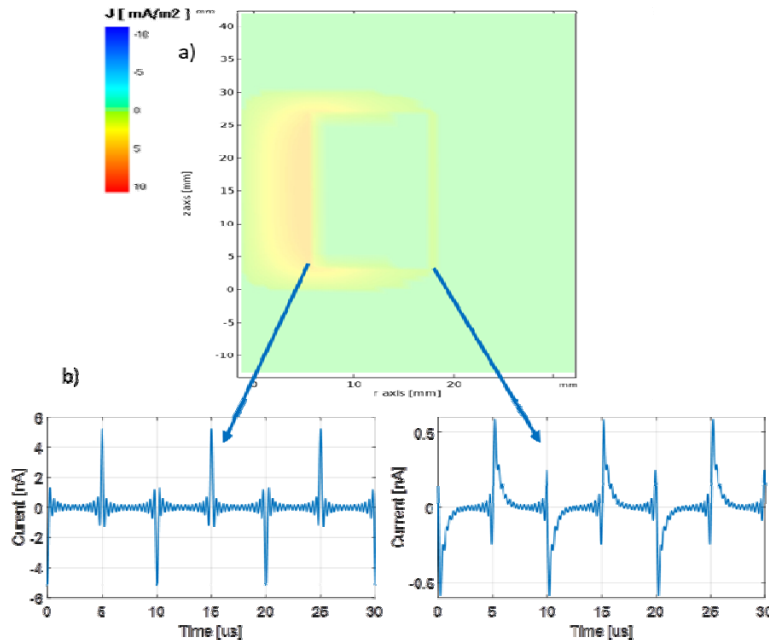


Fig. 7. Displacement current a) distribution for time $t = 5\mu s$, b) waveforms for selected elements in the ferrite core for $R_0 = 25\Omega$

Summary

In the paper, a novel approach to the Finite Element method has been presented. The numerical algorithm that combines the Fixed-Point Method and Harmonic Balance Method along with the Finite Element Method's multistage approach has been discussed. The Authors have also briefly presented and explained each numerical algorithm step. Proposed approach has been used to elaborate the field model of high-frequency transformer. The analysis was carried out under two distinct load conditions. The results indicate that variations in load value have a negligible effect on the distribution of displacement current. The displacement current distribution is found to be directly proportional to the electromotive force (EMF) values and the square of the supply frequency. Based on the conducted comparative analyses, it has been observed that the proposed method exhibits a shorter convergence time due to the parallel nature of computations. This feature is particularly noticeable during the analysis of areas in a saturated state composed of materials with nonlinear magnetization curve. The research indicated a 30% reduction in the convergence time of computations compared to the identical field model created in the commercial software Comsol Multiphysics.

The research presented in paper was supported by the statutory fund for young scientist of the Faculty of Control, Robotics and Electrical Engineering of the Poznan University of Technology (No. 0212/SBAD/0594)

Authors: mgr inż. Wojciech Ludowicz, Poznan University of Technology, Institute of Electrical Engineering and Electronics, ul. Piotrowo 3a, 60-965 Poznań, e-mail: wojciech.r.ludowicz@doctorate.put.poznan.pl. dr hab. inż. Rafał M. Wojciechowski prof. PP, Poznań University of Technology, Institute of Electrical Engineering and Electronics, ul. Piotrowo 3a, 60-965 Poznań, e-mail: rafal.wojciechowski@put.poznan.pl.

REFERENCES

- [1] Darwish, M.A.; Trukhanov, A.V.; Senatov, O.S.; Morchenko, A.T.; Saafan, S.A.; Astapovich, K.A.; Trukhanov, S.V.; Trukhanova, E.L.; Pilyushkin, A.A.; Sombra, A.S.B.; et al. Investigation of AC-measurements of epoxy/ferrite composites, *Nanomaterials*, 10 (2020), 492, doi:10.3390/nano10030492.
- [2] Jalaiah, K.; Mouli, K.C.; Krishnaiah, R.V.; Babu, K.V.; Rao, P.S.V.S, The structural, DC resistivity and magnetic properties of Zr and Co co-substituted Ni_{0.5}Zn_{0.5}Fe₂O₄. *Heliyon*, 5 (2019), e01800, doi:10.1016/j.heliyon.2019.e01800.
- [3] Hui, S.Y.R.; Zhong, W.; Lee, C.K., A Critical review of recent progress in mid-range wireless power transfer, *IEEE Trans. Power Electron*, 29 (2014), 4500–4511, doi: 10.1109/TPEL.2013.2249670.
- [4] Sanjari Nia, M.S.; Altimania, M.; Shamsi, P.; Ferdowsi, M., Magnetic field analysis for hf transformers with coaxial winding arrangements, *In Proceedings of the 2020 IEEE Kansas Power and Energy Conference (KPEC)*; IEEE: Manhattan, KS, USA, July 2020; pp. 1–5.
- [5] Maamar AET, Helaimi M, Taleb R., Analysis, simulation and experimental validation of high frequency DC/AC multilevel inverter. *Przeegląd Elektrotechniczny*; 96 (2020), no. 8: 16-19.
- [6] Achour, Y.; Starzyński, J., High-frequency displacement current transformer with just one winding, *COMPEL 2019*, COMPEL-10-2018-0414, doi:10.1108/COMPEL-10-2018-0414.
- [7] Biela, J.; Kolar, J.W., Using transformer parasitic for resonant converters - a review of the calculation of the stray capacitance of transformers, *In Proceedings of the Fourtieth IAS Annual Meeting. Conference Record of the 2005 Industry Applications Conference*; IEEE: Hong Kong, China; 3 (2005), pp. 1868–1875.
- [8] Hai Yan Lu; Jian Guo Zhu; Hui, S.Y.R., Experimental determination of stray capacitances in high frequency transformers, *IEEE Trans. Power Electron*, 18 (2003), 1105–1112, doi:10.1109/TPEL.2003.816186.
- [9] Zhang, X.; Zhao, Y.; Ho, S.L.; Fu, W.N., Analysis of wireless power transfer system based on 3D finite-element method including displacement current. *IEEE Trans. Magn.*, 48 (2012), 3692–3695, doi:10.1109/TMAG.2012.2196263.
- [10] Clemens, M.; Kähne, B.; Schöps, S., A Darwin time domain scheme for the simulation of transient quasistatic electromagnetic fields including resistive, Capacitive and Inductive Effects 2020.
- [11] Fang, N.; Liao, C.; Ying, L.-A., Darwin approximation to maxwell's equations, *In Computational Science – ICCS 2009*; Allen, G., Nabrzyski, J., Seidel, E., van Albada, G.D., Dongarra, J., Sloot, P.M.A., Eds.; *Lecture Notes in Computer Science*; Springer Berlin Heidelberg: Berlin, Heidelberg, 5544 (2009), pp. 775–784 ISBN 978-3-642-01969-2.
- [12] Ludowicz, W.; Wojciechowski, R.M., Analysis of the distributions of displacement and eddy currents in the ferrite core of an electromagnetic transducer using the 2d approach of the edge element method and the harmonic balance method, *Energies*, 14 (2021), 3980, doi:10.3390/en14133980.
- [13] Demenko, A., Eddy current computation in 3-dimensional models for electrical machine applications. *In Proceedings of the 2006 12th International Power Electronics and Motion Control Conference*; IEEE: Portoroz, August 2006; pp. 1931–1936.
- [14] Demenko, A.; Sykulski, J.K., Network equivalents of nodal and edge elements in electromagnetics, *IEEE Trans. Magn.*, 38 (2002), 1305–1308, doi:10.1109/20.996333.
- [15] Kuczmann, M., Nodal and edge finite element analysis of eddy current field problems, *Przeegląd Elektrotechniczny*, 84 (2008), no. 12, 2008, pp. 194-197.
- [16] Biro, O.; Preis, K., An efficient time domain method for nonlinear periodic eddy current problems, *IEEE Trans. Magn.*, 42 (2006), 695–698, doi:10.1109/TMAG.2006.871666.
- [17] Koczka, G.; Auberhofer, S.; Biro, O.; Preis, K., Optimal convergence of the fixed-point method for nonlinear eddy current problems, *IEEE Transactions on Magnetism*, 45 (2009), 948–951, doi:10.1109/TMAG.2009.2012477.
- [18] Wojciechowski, R.M.; Jedryczka, C., The analysis of stray losses in tape wound concentrated windings of the permanent magnet synchronous motor, *COMPEL*, 34 (2015), 766–777, doi:10.1108/COMPEL-10-2014-0287.